J. Automation & Systems Engineering 13-4 (2019): 106-116

Regular paper

A Photovoltaic Generator System Drive Forced Ventilation Greenhouse System

Faten Gouadria and L. Sbita

Research Unit of Photovoltaic, Wind and Geothermal Systems, National Engineering School of Gabes, University of Gabes, Tunisia

JASE
Journal of Automation & Systems Engineering

Abstract-This work describes a photovoltaic energy application which consists of fed electric power to a greenhouse ventilation system. Using this type of green source is aimed to reduce the agriculture production cost also recently; using this type of energy is becoming an alternative of the lack of electricity especially in isolated zone. This work deals with a new strategy which makes decisions on the connection modes between the photovoltaic generator, the battery bank and the BLDC motor-fan system.

The used method introduces an online energy management. The state of the three switches C_1, C_2 make decisions in which power can be delivered. The obtained results demonstrate the validation of the Energy Management algorithm used.

Keywords: Energy Management, Ventilation system, Anti-windup PI controller; , Brush-less DC Motor; Maximum Power Point Tracking (MPPT);

1. INTRODUCTION

WITH the depletion of fossil energy resources and their environmental problems caused during their exploitation, other alternative energy resources have been and must continue to be developed. Among them, we can mention the nuclear energy that does not directly reject carbon dioxide. However, the treatment of waste resulting from this method of production is very expensive. Another alternative is to exploit renewable energies, which offer the possibility to produce electricity properly.

Today, the most attention of green energies is the solar energy. There are two types of technology that employed solar energy, namely solar thermal and solar cell. A PV cell (solar cell) converts the sunlight into the electrical energy by the photovoltaic effect. Energy from PV modules offers several advantages, such as, requirement of little maintenance and no pollution. Recently, PV arrays are used in many applications, such as an agricultural system (such as ventilation, cooling system). PV module represents the fundamental power conversion unit of a PV generator system. The output characteristic of PV module is a function of the solar radiation and of the cell temperature. Since PV module has nonlinear characteristics, it is necessary to model it for the design and simulation of maximum power point tracking (MPPT)for PV system applications [1] and [2].Via the lack of energy in isolated site like agricultural one. Those green of energy can be used in different way heat, alimentation electrical installations (fan) in greenhouse system. To install electrical machine in greenhouse we look for a lower cost to facilated tasks for the responsible greenhouse and also we look for efficiency and validity of machine and methods used. The evolutions of control techniques have allowed the use of induction motors in the most of industrial applications. Later, induction motors are replaced by BLDC

motors that have a higher efficiency compared to induction motors, high speed, torque characteristics and small size. BLDC motor has simple structure and lower cost than other AC motors therefore it is used in variable-speed control of AC motor drives, [3]. In order to drive the BLDC motors, we have to use an inverter whose gate impulse is usually created from Hall engine tension extracted with Hall Effect sensors. The inverter fed a BLDC Motor who rotate with variable speed.. Many research in literature deals with the management of renewable energy systems [4]-[5][6]-[7]-[8]-[9]-[10]. This work we built a fuzzy controller of energy management of motor fan in charge of the ventilation system. In this paper, by taking a greenhouse measuring 16m wide by 50m long and having a volume of 2400m^3 following the guidelines cited in [11], this greenhouse should be ventilated with an air flow of about 48m^3.s−1. To achieve such a flow, a two fan should be used with a 1.27m diameter.

2. DEIGN OF THE PROPOSED MODEL

As display in Fig.1, the photovoltaic generator feeds the DC-DC boost converter. The IGBT switch of the boost converter is operated through a PandO algorithm controller such that the operation of the solar PV is optimized and the BLDC motor has a soft starting. Further, the boost converter feeds power to the voltage source inverter (VSI), supplying the BLDC motor coupled to a fan ventilator. Switching sequence for the voltage source inverter (VSI) is provided by the electronics commutation of BLDC motor. Electronic commutation is a process of decoding the Hall Effect signals generated by the inbuilt encoder of the motor according the position of rotor.

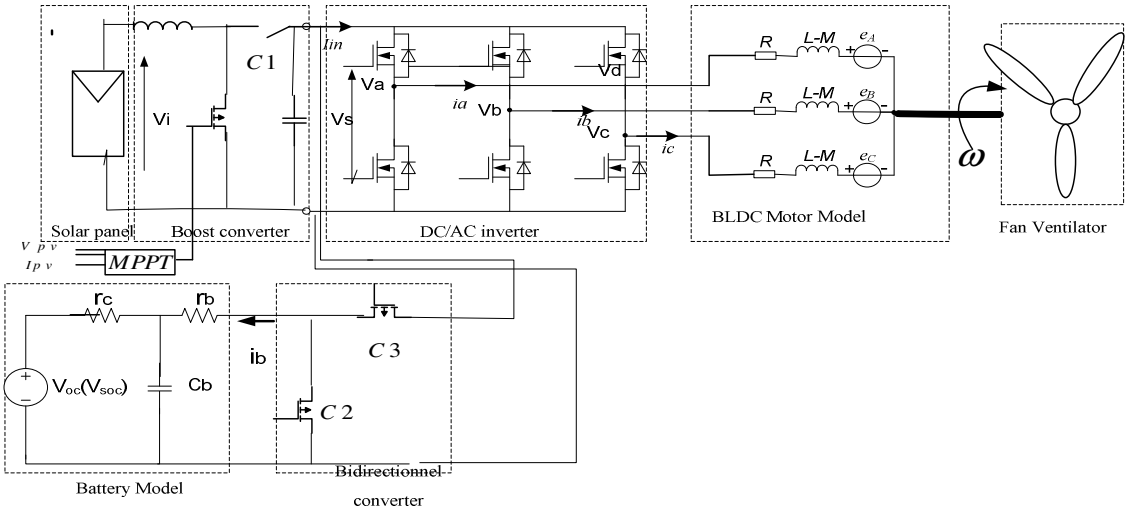

Figure 1 General Structure of the proposed generator fed -BLDC motor drive

Each stages of the proposed system are designed as follows:

2.1 PHOTOVOLTAIC GENERATOR

a. Electric model of a solar cell

A photovoltaic cell can be illustrated by its equivalent diagram as shown in the following figure.2:

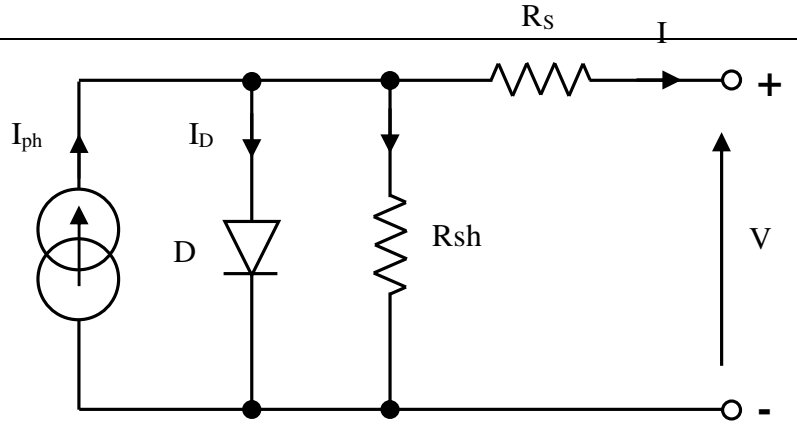

Figure 2 Equivalent circuit of solar cell

The cell has a bypass or shunt resistor (Rsh) characterizing the leakage current of the junction and a series resistance (Rs) representing the various resistances of contacts and connections.

By applying node law, we can write the following relation:

$$I = I_{ph} - I_D - I_{R_p} \tag{1}$$

$$I_{ph} = \frac{G}{1000}.\left(I_{CC(STC)} + k_i.(T - 298)\right) \tag{2}$$

And the current of the diode is can be expressed by:

$$I_D = I_0 \times (\exp^{\left(\frac{V + R_S \times I}{V_T}\right)} - 1) \tag{3}$$

The current inside the resistor is defined as below:

$$I_{R_p} = \frac{V + R_s \times I}{R_p} \tag{4}$$

So the equation can be written differently:

$$I = I_{ph} - I_0 \times (\exp^{\left(\frac{V + R_S \times I}{V_T}\right)} - 1) - \frac{V + R_s \times I}{R_p} \tag{5}$$

A PV module of ideal characteristics is such that is Rs null and Rsh becomes infinitely large. Hence the output current is described as bellow:

$$I = I_{ph} - I_0 \times (\exp^{\left(\frac{V}{\frac{k \times T_c}{q}}\right)} - 1) \tag{6}$$

There are many parameters that characterize a solar cell. These parameters can be determined from the characteristic equation, or current-voltage curves.

Among them the short circuit current (I_{CC}) (This is the current for which the voltage across the cell or the PV generator is zero). It can be determined as equation (7)

$$I_{cc} = I_{ph} - I_0 \times \left(\exp^{\left(\frac{R_S \times I_{cc}}{V_T} \right)} - 1 \right) - \frac{R_S \times I_{cc}}{R_p} \tag{7}$$

For most solar cells (whose series resistance is low), we can neglect the term $I_0 \times \left(\exp^{\left(\frac{R_S \times I_{cc}}{V_T} \right)} - 1 \right)$ compare to I_{ph} so we can rewrite Icc as follow $I_{cc} = \frac{I_{ph}}{1 + \frac{R_S}{R_p}}$ In the ideal case (Rs null and infinite Rp), the current I_{CC} merges with the photo-current Iph. The second parameter is the Open circuit voltage (Voc) (it is the voltage for which the current delivered by the photovoltaic generator is zero (it is the maximum voltage of a photocell or a photovoltaic generator)

$$0 = I_{ph} - I_0 \times \left(\exp^{\left(\frac{V_{co}}{V_T} \right)} - 1 \right) - \frac{V_{co}}{R_p} \tag{8}$$

In the ideal case, its value is slightly lower than:

$$V_{co} = V_T . \ln\left(\frac{I_{ph}}{I_0} + 1 \right) \tag{9}$$

The third parameter is the form factor and it can be defined as the ratio between the maximum value of the extractable power (Vpm Ipm) of the photocell under the standardized measurement conditions, and the product (Voc, Icc). The forth term is the fill factor and it is defined as the ratio between the maximum power delivered by the cell and the incident light power.

$$FF = \frac{V_{pm} \times I_{pm}}{I_{cc} \times V_{co}} \tag{10}$$

With:

G; is the solar radiation/m2

$I_{CC(STC)}$; Short-circuit current at Standard Operating Conditions (STC) set by 1000 W/m2 and T=25 ° C

k_i ; is coefficient of influence the temperature on the current in (A/°K),
T; is the temperature of the cell (°K).
I_{ph} ; Represents the photo-current created in solar cells by solar radiation,
I_D ; Represents the current of the diode in the dark,
I, V; Represent current and cell voltage.
Ns; is the number of cell connected en series,
A; is the ideality factor,
Tc; is the actual cell temperature,
I0; is the reverse saturation current of the diode (A),
K; Boltzmann constant (1.381×10^{-23} J/K),
Q; electron charge(1.06×10^{-19} C),
VT; is the thermal voltage because dependant of temperature.

2.2 MODELING OF DC/DC CONVERTER TYPE BOOST

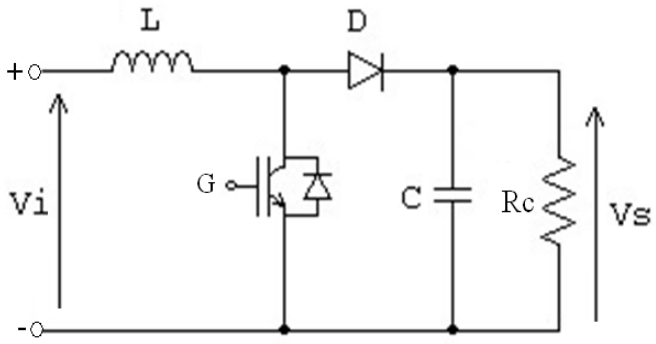

Figure 3 Equivalent circuit of Boost

A chopper is a static converter that provides an adjustable average voltage value from a fixed DC voltage.
For a boost converter, the inductor stores energy is for a time equal to αTs (Ts is the switching period of the switch and α duty cycle). Indeed, we have:

$$V_L = V_i = L \times \frac{dI_L}{dt} \tag{11}$$

The energy is then returned to the load during:

$$V_i - V_0 = L \times \frac{dI_L}{dt} \tag{12}$$

So the DC voltage transfer function can be written as:

$$\frac{Vs}{Vi} = \frac{1}{1 - D} \tag{13}$$

With Vi is converter input voltage (the output voltage of the PV array) Vs is the output voltage, D is the duty ratio of the controllable switch. The boost converter operates in the continuous conduction mode for L > Lmin where:

$$L_{\min} = \frac{(1-D)^2 DR}{2f} \tag{14}$$

With, f is the switching frequency and R is the load resistance. The minimum value of the filter capacitance that results in voltage ripple Vr is given by:

$$C_{\min} = \frac{Dv_d}{V_r Rf} \tag{15}$$

2.4 STORAGE MODELING

Like shown in fig.1, the battery is modeled as a capacitor C_b connected in series with her internal resistance rb. Since Cb is sufficiently large, the terminal voltage of the battery, vbat , can be calculated as presented :

$$v_{bat} = V_{oc} - i_b . r_b \tag{16}$$

Then the transfer function between the battery current ib and the duty cycle d_1 of the switch S_1 in the charge mode can be written as follow:

$$F_c(s) = \frac{i_b(s)}{d_1(s)} = \frac{(v_{pv} - v_b).(s + \frac{1}{r_b . c_1})}{s^2 + (\frac{r_2}{l_1} + \frac{1}{r_b . c_1})s + \frac{r_1 / r_b + d_1}{l_1 . c_1}} \tag{17}$$

Where v_{pv} and v_b represent the average voltages of the PV panel and the battery, respectively; r2 and r_b represent the parasitic resistance of the inductor l_2 and the internal resistance [6].

The same procedure can be used to determine the discharge mode, so the transfer function between ib and the duty cycle d2 of the switch S2 in the discharge mode is:

$$F_{dis}(s) = \frac{i_b(s)}{d_1(s)} = \frac{v_{pv} . (s + \frac{1}{r_b . c_1})}{s^2 + (\frac{r_2}{l_1} + \frac{1}{r_b . c_1})s + \frac{r_1 / r_b + 1}{l_1 . c_1}} \tag{18}$$

In order to control the current of the battery, a proportional-integral (PI) controller is used in the charge/discharge mode separately, as shown in Fig.4. The battery current PI controller takes the current error as the input to generate the duty cycle for C1 or C2 in the charge or discharge mode, respectively.

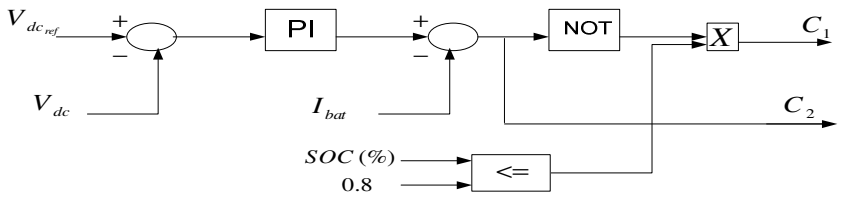

Figure 4 Equivalent circuit of control charge and discharge battery

2.4 BRUSHLESS DC MOTOR DRVES

The BLDC motor rotor has a permanent magnet rotating at the same frequency with the presence of a classic three phase stator like that of a synchronous motor. BLDC drive needs variable frequency and variable amplitude excitation that is can be provided by a three phase full bridge inverter. The principal role of this inverter in the electric circuit is the current regulation and the electronic commutation.

The Hall element is the most commonly used position sensor for detecting the rotor position of the BLDC motor. The simplified model can be represent in fig.1 where V_a, V_b, V_c are represent the armature voltages I_a, I_b , I_c are the armature currents; R is the resistance of the armature windings; e_a, eb, ec are the back emf; M and L are the mutual-inductance and self inductance of the winding respectively. For the the position of the rotor is directly deduced from the mechanical position of the rotor which is measured by the sensor the equation [8][9]:

$$\theta_e = P.\theta_r \tag{19}$$

Where P is the number of motor pairs of poles, therefore, the expression of the electric speed is valued as:

$$\omega_e = \frac{d\theta_e}{dt} = p.\frac{d\theta_r}{dt} \tag{20}$$

Inductances and mutual are constant for the type where the permanent magnets mounted on the surface of the cylindrical rotor, case when the windings are symmetrical, the own inductances are identical given by:

$$L_{aa} = L_{bb} = L_{bc} = L \tag{21}$$

And the mutual inductances are also identical given by:

$$M_{db} = M_{ba} = M_{ac} = M_{ca} = M_{bc} = M_{ca} = M \tag{22}$$

For a symmetrical three-phase winding and a balanced system, the voltages across the three phases are given in the matrix by:

$$\begin{bmatrix} V_a \\ V_b \\ V_c \end{bmatrix} = \begin{bmatrix} R & 0 & 0 \\ 0 & R & 0 \\ 0 & 0 & R \end{bmatrix} \begin{bmatrix} i_a \\ i_b \\ i_c \end{bmatrix} + \frac{d}{dt} \left(\begin{bmatrix} L.i_a + M\ (i_b + i_c) \\ L.i_b + M\ (i_a + i_c) \\ L.i_c + M\ (i_a + i_b) \end{bmatrix} \begin{bmatrix} i_a \\ i_b \\ i_c \end{bmatrix} \right) + \begin{bmatrix} e_a \\ e_b \\ e_c \end{bmatrix} \tag{23}$$

Since the stator windings are star-connected, the sum of the three currents of phase is set to zero:

$$i_a + i_b + i_c = 0 \tag{24}$$

Therefore, the voltage takes the following form:

$$\begin{bmatrix} V_a \\ V_b \\ V_c \end{bmatrix} = \begin{bmatrix} R & 0 & 0 \\ 0 & R & 0 \\ 0 & 0 & R \end{bmatrix} \begin{bmatrix} i_a \\ i_b \\ i_c \end{bmatrix} + \frac{d}{dt}\left(\begin{bmatrix} (L\text{-}M) & 0 & 0 \\ 0 & (L\text{-}M) & 0 \\ 0 & 0 & (L\text{-}M) \end{bmatrix} . \begin{bmatrix} i_a \\ i_b \\ i_c \end{bmatrix} \right) + \begin{bmatrix} e_a \\ e_b \\ e_c \end{bmatrix} \tag{25}$$

With:

$e_a = k_{ee}.w_r.f_a(\theta_e)$, $e_b = k_{ee}.w_r.f_b(\theta_e)$ and $e_c = k_{ee}.w_r.f_c(\theta_e)$ are the respectively is the electromotive force of phase a, b and c respectively; k_{ee} is the coefficient of the electromotive force; $f_a(\theta_e)$ $f_b(\theta_e)$ $f_c(\theta_e)$ are functions that depend solely on the rotor position.

The electromechanical torque is valued as:

$$T_{em} = J.\frac{d\omega_r}{dt} + B.\omega_r + T_L \tag{26}$$

Where J is the moment of inertia, T_L and T_c, are load and cogging torques, and B is the damping constant. But T_{em} for three phases BLDC motor is dependent on the speed, the current and the back-EFM wave forms, so the electromagnetic torque value is given by [10][11]:

$$T_{em} = \frac{1}{\omega_m}.(e_a.i_a + e_b.i_b + e_c.i_c) \tag{27}$$

In the case where the BLDC drives ventilator, the load torque is proportional to the square of the speed:

$$T_L = k.\omega^2 \tag{28}$$

Rated torque of motor is calculated as:

$$T_r = \frac{P}{\omega_s} \tag{29}$$

Where P is motor power in watts, ω_S is synchronous speed in rad/s. Constant k is calculated using the two previous equations.

In order to control the speed bldc motor a windup PI controller is used. Actual speed is compared with reference speed command and error is controlled by an Anti-windup PI controller whose output is the duty cycle. Duty cycle in converted in PWM by comparing the duty cycle voltage with saw tooth waveform.

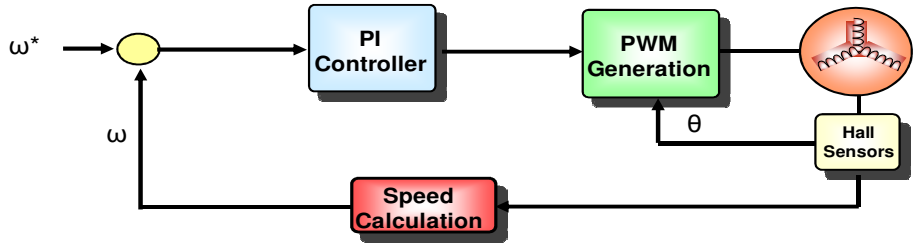

Figure 4 The block of Closed loop controller for speed for the BLDC motor

6. RESULT AND INTERPRETATIONS

All parameters used in the simulation are presented in table.1.
The simulation is carried out with MATLAB/SIMULINK and the meteorological data needed are presented in fig.5 and fig.6.

TABLES1. ELECTRICAL MOTOR PARAMETERS

Parameter	Value
Rated Power	2.2 kW
Number of phases	3
Rated Speed	1650 rpm
Pole Number	4
Armature Inductance	8.5 mH
Armature Resistance	2.875 Ω
Rotor Inertia	0.8 e^{-3} Kgm^2
Damping constant	1 e^{-3} N.m.s/rad
Back EMF constant	0.175 V.Sec

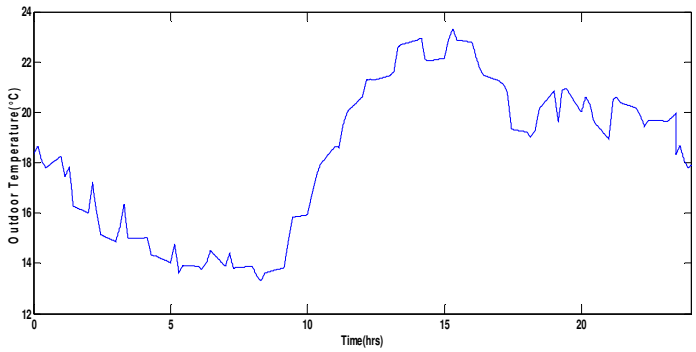

Figure 5 Outdoor temperatures (°C)

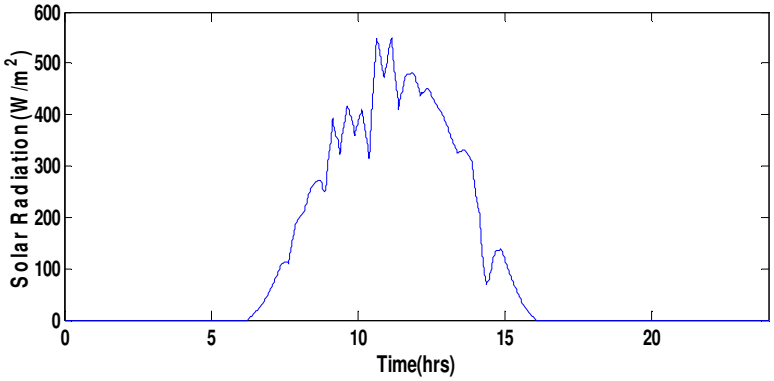

Figure 6 Solar Radiation (W/m^2)

To validate the DC part models, we need to check the key variables of his part. We can see that the DC bus voltage of the converter output voltage track the right value 500V. So the algorithm attaints the considered goal to aliment our charge.

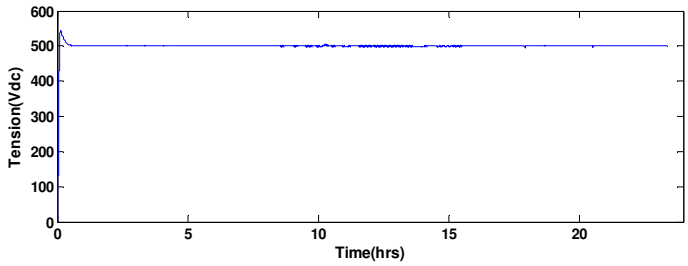

Figure 7 Bus DC Voltage (V)

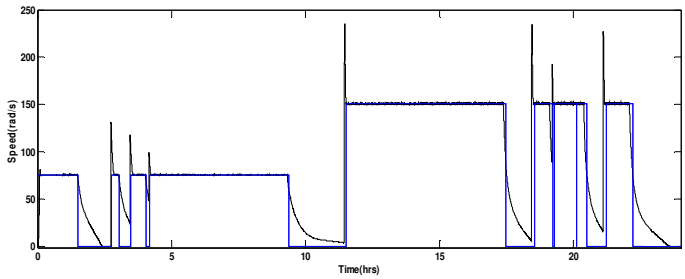

Figure 8 The BLDC Motor speed vs the reference speed

Precise speed control of BLDC motor is complex due to non-linear relation between the winding currents and the rotor speed. For a very slow, medium, fast and precise speed response, a fast track of the set speed is important, which maintains the insensitivity to the variations of parameters. Currently, the presented controller handles these control issues. In addition, this controller is very sensitive to control speed change, parameter variation, and load disturbances. With higher frequency switching, The BLDC motor runs at a higher speed.

7. CONCLUSIONS

In this work the development of PI controller for the BLDC motor is accepted out. The effectiveness and robustness of the developed speed controller are evaluated under various operating conditions of the PV system (solar irradiation, the temperature of outside weather). The transient performances of the controller are investigated while varying the reference speed and load torque (relied of the fan system situation and the conditions of the weather of values. The use of green energy as a source help us to ensure effective and

efficient working of the BLDC Motor Fan, since nowadays the BLDC motor is used in several applications. The work provides the development of the MPPT method which provided the use of such a higher rating motor with ease and with the successful operation of the motor.

ACKNOWLEDGMENT

The authors are very grateful to the Tunisian Ministry of Higher Education and Scientific Research TMHESR by the support of the research Unit which code UR11ES82.

REFERENCES

[1] C. Qi and Z. Ming, "Photovoltaic Module Simulink Model for a Stand-alone PV System," Phys. Procedia, vol. 24, pp. 94–100, 2012.

[2] H. Tsai, C. Tu, and Y. Su, "Development of Generalized Photovoltaic Model Using MATLAB / SIMULINK," Proc. World Congr. Eng. Comput. Sci. 2008 WCECS 2008, Oct. 22 - 24, 2008, San Fr. USA, p. 6, 2008.

[3] A. Halvaei Niasar, A. Vahedi, and H. Moghbeli, "Torque control of brushless DC motor drive based on DSP technology," Electr. Mach. Syst. 2007. ICEMS. Int. Conf., pp. 524–528, 2007.

[4] H. Yatimi, E. Aroudam, and M. Louzazni, "Modeling and Simulation of photovoltaic Module using MATLAB / SIMULINK Modélisation et Simulation du Module photovoltaïque sous MATLAB / SIMULINK," vol. 8, pp. 3–7, 2014.

[5] B. S. Borowy and Z. M. Salameh, "Methodology for optimally sizing the combination of a battery bank and PV array in a Wind/PV hybrid system," IEEE Trans. Energy Convers., vol. 11, no. 2, pp. 367–373, 1996.

[6] J. Zeng, W. Qiao, and L. Qu, "An Isolated Three-Port Bidirectional DC #x2013;DC Converter for Photovoltaic Systems With Energy Storage," IEEE Trans. Ind. Appl., vol. 51, no. 4, pp. 3493–3503, 2015.

[7] R. Akkaya, A. A. Kulaksiz, and Ö. Aydoğdu, "DSP implementation of a PV system with GA-MLP-NN based MPPT controller supplying BLDC motor drive," Energy Convers. Manag., vol. 48, no. 1, pp. 210–218, 2007.

[8] S. Systems, S. Nagapavithra, and S. Umamaheswari, "Fuzzy Based Power Factor Correction for Bldc Motor Using Hybrid Inverter," no. March, pp. 3–4, 2017.

[9] P. D. T. C. B. M. D. with kalman F. A. pdfrakas. Salawria, R. S. Lodhi, and P. Nema, "Implementation of PSO-Based Optimum Controller for Speed Control of BLDC Motor," 2017.

[10] D. S. Nair, G. Jagadanand, and S. George, "Sensorless Direct Torque Controlled BLDC Motor Drive with Kalman Filter Algorithm," pp. 2160–2165, 2017.

[11] A. Movahedi and G. Shahgholian, "Design and smulation of sensorless BLDC motor drive using DTC and SWF," ECTI-CON 2017 - 2017 14th Int. Conf. Electr. Eng. Comput. Telecommun. Inf. Technol., no. 1, pp. 895–898, 2017.

.